ORIGINAL ARTICLE

Design, Formulation and Characterization of Solid-lipid Nanoparticles for Anti-retroviral Drug

Anita H. Pagar, Ashish Y. Pawar, Santosh R. Tambe

Department of Pharmaceutics, Mahatma Gandhi Vidyamandir's Pharmacy College (Affiliated to Savitribai Phule Pune University, Pune), Nashik, Maharashtra, India

Abstract

Background: Treating human immunodeficiency virus (HIV)/acquired immunodeficiency syndrome effectively remains a significant challenge due to issues, such as low absorption, frequent dosing, and side effects associated with traditional antiretroviral drugs. This study focuses at solid lipid nanoparticles (SLNs) as a new way to deliver drugs. These nanoparticles could provide better control over how these drugs are absorbed and released in the body, making treatment more manageable for patients. **Materials and Methods:** We made SLNs utilizing ultrasonication and high-shear homogenization. A commonly used antiretroviral drug was embedded in a lipid matrix made from glyceryl monostearate and stabilized with Poloxamer 188. Researchers carefully evaluated these nanoparticles for key properties, such as the size of the particles, the size distribution polydispersity index (PDI), and the surface charge (zeta potential), drug retention (entrapment efficiency), and the timing of drug release in lab tests. **Results:** The resulting SLNs had an average particle size of <200 nanometers and a PDI of <0.3, which means that the size distribution was even. The zeta potential readings showed that the formulation was stable and that drug retention was high, at more than 80%. The *in vitro* release investigation indicated that the drug was released slowly over a whole 24-h period, which suggests that it could have long-lasting effects. **Conclusion:** These results show that SLNs could make antiretroviral medications work better in the body. They offer more stable and sustained release and may reduce how often patients need to take their medication. By simplifying dosing and enhancing drug performance, SLNs could play a key role in making HIV treatment more effective and patient-friendly.

Key words: Dolutegravir solid lipid nanoparticles, high-pressure homogenization, human immunodeficiency virus -1 infection, solid lipid nanoparticles

INTRODUCTION

Solid lipid nanoparticles (SLN) are mostly made up of lipids that are solid at room temperature and surfactants that help mix them together. For colloid drug delivery, the average size of these particles is between 50 and 1000 nm.[1] SLNs have special features such being small, having a huge surface area, being able to hold a lot of drugs, and having phases interact at the interfaces. They are interesting because they could make drugs, nutraceuticals, and other materials work better.[2] There are several ways to make SLN, including high-pressure homogenization.[3] We have created and thoroughly tested SLN formulations for a number of ways to use them, including parenteral, oral, cutaneous, ophthalmic, pulmonary, and rectal.[4] SLN are colloidal dispersions in water that are made up of solid, biodegradable lipids.[5] SLNs have the best features of various colloidal carriers in their class and none of their bad ones, namely, physical stability, keeping labile medicines from breaking down, regulated release, and great tolerability.[6] Dolutegravir (DTG) is an INSTI that is authorized to treat human immunodeficiency virus (HIV-1) infection. It is a second-generation integrase strand transfer inhibitor. Despite its potent antiviral activity, DTG exhibits limitations, such as low aqueous solubility and poor oral bioavailability, characteristic of Bio-pharmaceutics Classification System Class II drugs. Because of these problems, new drug delivery systems need to be devised

Address for correspondence:
Anita H. Pagar, Department of Pharmaceutics, MGV'S Pharmacy College, Panchavati, Nashik - 422 003, Maharashtra State, India. Phone: +91-9860743860.
E-mail: anu.h.pagar@gmail.com

Received: 19-05-2025
Revised: 24-06-2025
Accepted: 30-06-2025

to make it more effective as a treatment. Many people are interested in SLNs as possible carriers for medications that are both lipophilic and hydrophilic, such as antiretroviral treatments, such as DTG.

Some benefits of SLNs include that they can control medication release, make pharmaceuticals more stable, and hold both lipophilic and hydrophilic compounds, including antiretroviral agents, such as DTG. SLNs offer advantages, such as controlled drug release, improved stability, and the ability to encapsulate both lipophilic and hydrophilic drugs, thereby enhancing their bioavailability.[7,8] The formulation of DTG into SLNs aims to overcome its solubility and bioavailability issues, thereby improving its therapeutic outcomes in HIV treatment. Recent studies have focused on optimizing the formulation of DTG-loaded SLNs using various techniques, such as hot homogenization followed by ultrasonication. For instance, a study by Prasanth *et al*. utilized a 3^2 full factorial design to prepare DTG-loaded SLNs, obtaining formulations with the smallest possible particle size, the best zeta potential, and the highest drug encapsulation efficiency.[7] The study also showed how the content of lipids affects the physical and chemical properties of nanoparticles. Furthermore, the use of biocompatible and biodegradable materials in SLN formulations has been explored to ensure safety and efficacy. For example, chitosan-based SLNs have been developed for pediatric HIV therapy, demonstrating improved stability and drug release profiles compared to pure DTG. These formulations also exhibited enhanced cellular uptake and antiretroviral activity, indicating their potential for improving treatment adherence in children.[9,10] The incorporation of SLNs into thermo sensitive gels has also been investigated for vaginal delivery systems, aiming to provide sustained drug release and improved adherence to mucosal surfaces. Studies have shown that DTG-loaded SLNs in thermo sensitive gels exhibit controlled drug release and maintain stability under physiological conditions, suggesting their potential for pre-exposure prophylaxis in HIV prevention. In short, converting DTG into SLNs is a promising way to improve its solubility, bioavailability, and therapeutic effectiveness. Researchers are still working to make these formulations better so that they can better deal with the problems that come with treating and preventing HIV.[11]

SLNs have come to light as promising carriers that can get around these problems. SLNs are tiny colloidal carriers made of solid lipids that are safe for living things and are kept stable by surfactants. They have benefits such regulated medication release, preservation of unstable pharmaceuticals, and the capacity to hold both water-loving and water-hating molecules.[12]

MATERIALS AND METHODS

DTG was obtained from Cipla Ltd. Situated at Lbs., Merg, vikhroli west Mumbai, Maharashtra India. The Phospholipon 90 H was obtained as gift sample from Chemet, Santacruz (West), Mumbai. Polymers were procured, such as polyvinyl alcohol, polyethylene glycol, and Tween 80 From Merck Life Science Pvt. Limited, Navi Mumbai, India.

Methods

Method of preparation

We made SLN by first heating them up and then using ultrasonication (Labline). In short, 50 mg of DTG was carefully weighed and added to Phospholipon 90 H, which had been melted at 80°C. We blended Tween 80 with double-distilled water to form a 0.5% and 1% solution. Then we heated it in a beaker to 80°C. The hot aqueous surfactant solution was added to the hot lipid phase when the lipid phase was clear and even. The two stages were mixed together at 1000 rpm for 30 min using a high-speed homogenizer (REMI).

The temperature stayed at 80°C while the homogenization was going on. We used a probe sonicator (Misonix 3000) at 100W for 3 min to ultrasonify the pre-emulsion we received. The temperature of production was set at least 5°C higher than the melting point of the lipids to stop recrystallization during homogenization and ultrasonication. The nanoemulsion (o/w) was cooled in an ice bath to make SLN, and then it was diluted with deionized water to make 200 mL. We kept the SLN dispersions at 4°C so we could do more tests on them.[13,14]

Experimental design

We used the response surface methodology (RSM) to build and study the polynomial models using the Quality by Design approach, which required fewer experimental runs. Box-Behnken A design with three factors and two levels was used to look at the quadratic response surfaces by looking at how distinct independent variables affected different dependent variables. Y1, Y2, and Y3 were the codes for the percentage of drug content, the percentage of drug release, and the percentage of drug entrapment. Three independent variables, namely, Phospholipon 90 H (A), tween 80, and homogenization speed (C) (rpm), were chosen. There were two levels of each variable, called high and low. Table 1 shows all the finished independent variables and response variables and detailed batches are discussed in Table 2.

Table 1: List of independent and dependent variables in the box–Behnken design

Independent variables	Low value (-1)	High value (+)
Phospholipon 90 H (A) (mg)	100	400
Tween 80 (B) (%)	0.5	1
Homogenization speed (rpm)	1000	2000
Dependent variables	Constraints	
Drug Content (%)	Maximize	
Entrapment efficiency (%)	Maximize	
Drug release (%)	Maximize	

Table 2: DOE suggested and experimental batches

Formulation code	Dolutegravir (mg)	Phospholipon 90 H (mg)	Tween 80 (%)	Homogenization speed (rpm)	Methanol
PF1	50	250	0.75	1500	10
PF2	50	250	1	1000	10
PF3	50	250	1	2000	10
PF4	50	100	0.5	1500	10
PF5	50	400	0.5	1500	10
PF6	50	250	0.5	2000	10
PF7	50	100	1	1500	10
PF8	50	250	0.5	1000	10
PF9	50	400	1	1500	10
PF10	50	100	0.75	1000	10
PF11	50	400	0.75	2000	10
PF12	50	100	0.75	2000	10
PF13	50	400	0.75	1000	10

Characterization of solid-lipid nanoparticle

Drug content

Use a pipette to measure 100 µL of SLN formulation and put it in a 10 mL volumetric flask.

To get the right concentration for UV analysis, add methanol to the solution until it is 10 mL. To get rid of any solid particles, pass the diluted solution through Whatman filter paper No. 1 or a membrane filter that works well. Use a UV spectrophotometer (Jasco V-630) to find out how much light the filtered solution absorbs at the drug's wavelength of 259 nm.[15]

Entrapment efficiency (EE%)

We put 10 mg of SLN formulation in a volumetric flask and then added methanol to generate 10 mL. The fluid that had been diluted was poured into Eppendorf tubes and spun for 2 h at 4°C at 10,000 rpm. Carefully gathered and filtered the supernatant. The filtered sample was analyzed by UV (Jasco Uv-630) at 259 nm to get the drug present in supernatant.[16,17]

$$\text{Entrapment efficiency (\%)} = \frac{\text{Added drug} - \text{Free drug}}{\text{Added}} \times 100$$

In vitro dissolution study

We used a USP Type II (paddle) dissolving device to do *in vitro* drug release investigations to see how the SLNs released their drugs. Each formulation included the same quantity of medication as 50 mg and was mixed with 900 mL of phosphate buffer with a pH of 6.8. The dissolving medium was kept at a constant temperature of 37 ± 0.5°C and agitated with a paddle at a speed of 100 rpm for 24 h. Five milliliters of the dissolution medium were taken for examination at certain times, such as 1, 2, 3, 4, 5, 6, 7, and 8 h. We used a UV-Visible spectrophotometer (Jasco UV-630) to look at these samples at a wavelength of 259 nm to see how much medication was released over time.[18]

Particle size, polydispersity index (PDI) and zeta potential

The 10 mg SLN formulation was combined with distilled water and sonicated for 30 min. The test was done at 25°C. The same steps were taken at the zeta potential.[19]

Fourier transform infrared (FTIR) spectroscopy

FTIR was used to do the study of drug excipients compatibility. The optimized batches PF13 samples were scanned with the diffraction reflectance scanning technique over a wave number range of 500–4000/cm.[20]

Differential scanning calorimetry (DSC)

We used a modulated DSC (Mettler Toledo, SW STARe, and USA) to undertake DSC experiments. We weighed the optimized batch PF13 (2–8 mg), put it in aluminum pans, and sealed them with lead. The temperature went up steadily at a rate of 10°C/min in a nitrogen environment (50–60 mL/min), and the heating range was 50–250°C. The thermograms of the formulation that came out were collected.[21]

X-ray diffraction (XRD) study

We used the data from XRD to find out if the novel compounds were crystalline or amorphous. The settings for the experiment

were 40 kV voltage, 30 mA current, and target metals Cu and filter K. We scanned optimized batch PF3 samples over a 2° range of 10–90°C with a phase scale of 0.2°.[22]

Scanning electron microscopy (SEM)

SEM (Carl Zeiss, supra55, Germany) at the central instrumental facility (YCIS SATARA). Photographs of samples were taken by a different magnification power (×50,000). We utilize electron microscopy to look at the shape, surface topography, and texture of broken things. The surface morphology of optimized batches was determined.[23]

Stability study

The temperature and humidity conditions for all SLNP samples were kept at 4°C ± 1°C (60% RH) in a stability chamber for 3 months. This was based on past research with some small changes. We checked the medication content, EE, and drug release once a month.[24,25]

RESULTS AND DISCUSSION

Drug content

The drug content of formulations PF1 to PF13 showed considerable variation, reflecting the efficiency of drug loading across different batches. PF3 demonstrated the highest drug content at 97.34 ± 0.36%, indicating excellent drug incorporation and formulation consistency. This was closely followed by PF5 (96.02 ± 0.01%) and PF9 (94.42 ± 0.02%), which also showed high drug loading efficiency. Formulations, such as PF1 (79.29 ± 0.02%) and PF10 (83.78 ± 0.04%) exhibited the lowest drug content, suggesting potential inefficiencies in formulation or drug incorporation processes. Overall, the data highlights PF3 as the most optimal formulation in terms of drug content, supporting its selection for further evaluation and development. The batch-wise results are mentioned in Table 3. The 3D surface and contour plots show how Phospholipon 90H and Tween 80 interact to affect drug content. The drug content was lowest at the mid-range concentrations of both substances and highest at their upper levels, which indicates a combined effect. The graphical representation of the results shown in Figure 1 back up the batch data and highlight PF3 as the best formulation with the highest drug loading efficiency.

Table 3: Drug content (%) of PF1–PF13

Formulation code	Drug content (%)
PF1	79.29±0.02
PF2	88.38±0.14
PF3	97.34±0.36
PF4	86.68±0.85
PF5	96.02±0.01
PF6	86.54±0.89
PF7	93.66±0.35
PF8	88.8±0.47
PF9	94.42±0.02
PF10	83.78±0.04
PF11	93.36±0.14
PF12	87.02±0.03
PF13	87.54±0.04

Table 4: Entrapment efficiency (%) of PF1–PF13

Formulation code	Entrapment efficiency (%)
PF1	71.24±0.124
PF2	88.06±0.05
PF3	93.94±0.63
PF4	81.24±0.75
PF5	85.1±0.09
PF6	82.74±0.04
PF7	89.9±0.14
PF8	85.18±0.09
PF9	88.66±0.63
PF10	79.56±0.48
PF11	88.86±0.04
PF12	79.24±0.09
PF13	83.1±0.48

EE%

The effectiveness of formulations PF1 to PF13 at trapping things was very different, indicating the impact of formulation composition on drug encapsulation. Among all, PF3 exhibited the highest EE% at 93.94 ± 0.63%, highlighting its superior capability to encapsulate the drug effectively. The batch-wise results are mentioned in Table 4. Other formulations, such as PF7 (89.9 ± 0.14%), PF11 (88.86 ± 0.04%), PF9 (88.66 ± 0.63%), and PF2 (88.06 ± 0.05%) also showed relatively high efficiencies, suggesting favorable formulation characteristics. In contrast, PF1 displayed the lowest EE% (71.24 ± 0.124%), indicating suboptimal encapsulation. Overall, PF3 emerged as the most efficient formulation, making it the most suitable candidate for further development and evaluation. The 3D surface and contour plots in Figure 2 shows that EE% was lowest at mid-levels of Phospholipon 90H and Tween 80, as seen in batches, such as PF1 and PF6. Higher concentrations of both excipients led to improved efficiency, with PF3, PF7, and PF11 showing maximum drug encapsulation.

In vitro dissolution study

The *in vitro* drug release characteristics of formulations PF1 to PF13 revealed notable differences in release behavior over an

8-h period. Among the first group (PF1–PF6), PF3 exhibited the highest cumulative drug release of 97.09%, indicating it as the most effective formulation in terms of sustained and complete drug release. PF3 also demonstrated a consistently higher release rate across all time points compared to the others, supporting its selection as the optimized batch. Similarly, in the second group (PF7–PF13), formulations, such as PF10, PF11, and PF12 showed significant drug release, reaching over 90% by the 8th h. However, PF3 still outperformed all in terms of both the amount and consistency of release. These results suggest that PF3 provides a more controlled and efficient drug delivery profile, making it the best choice for more research and clinical testing [Table 5 and Figure 3].

Kinetic analysis of drug release

We used kinetic equations models to fit the *in vitro* release data for the optimized batch (PF3) to determine the release mechanism that best fits the release pattern.

We used the Higuchi, zero, and first-order models as kinetic equations. The graphs below show the values of the kinetic rate constant (k) and the determination coefficient (R2). We used zero-order, first-order, and Higuchi models to find out how the medication was released from the improved formulation PF3. The zero-order model had the highest correlation coefficient (R^2 = 0.9768) of these indicating that

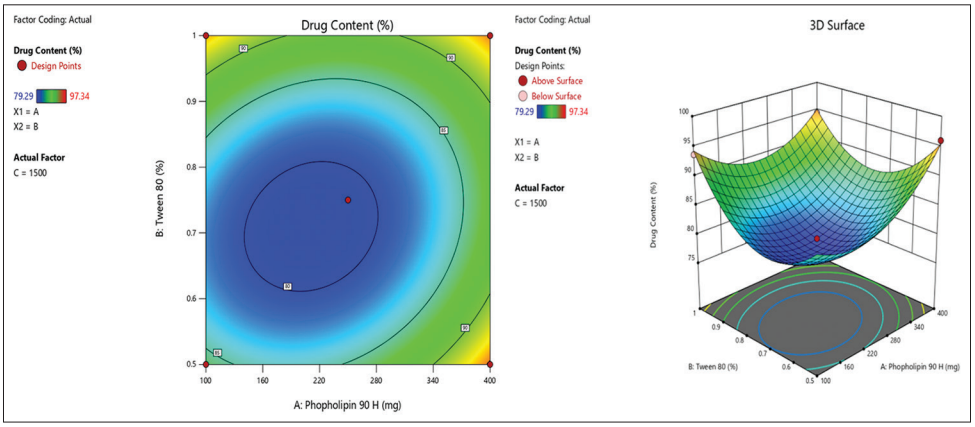

Figure 1: Counter and 3D surface plots of drug content

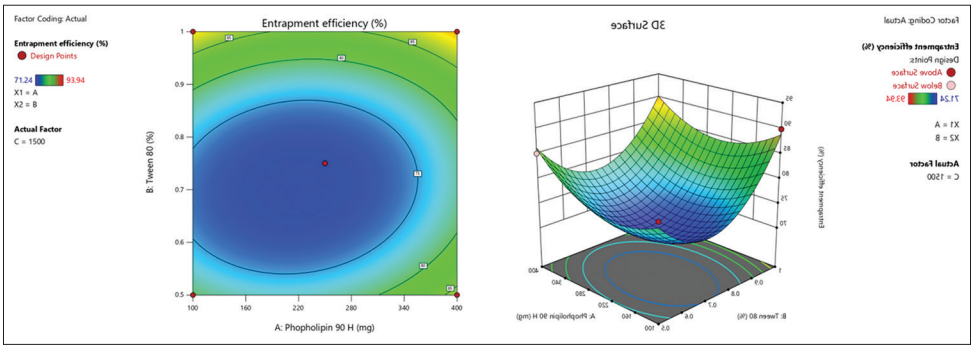

Figure 2: Counter and 3D surface plots of entrapment efficiency

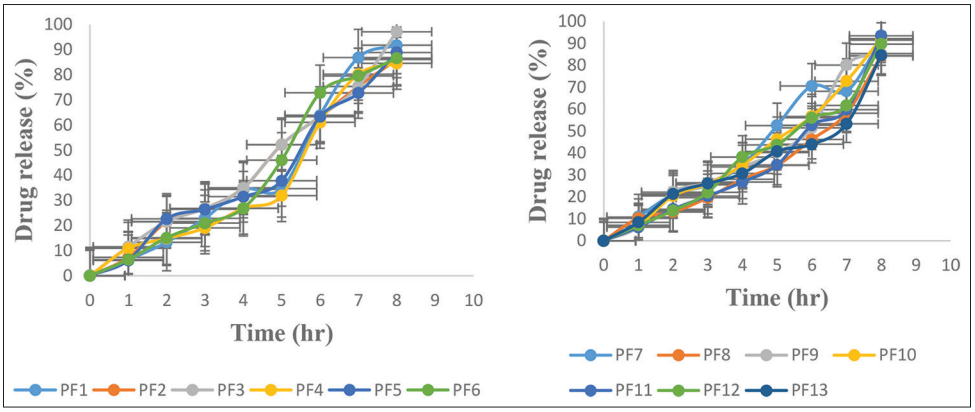

Figure 3: Drug release of PF1–PF13

PF3 follows a zero-order release pattern, where the medicine comes out at a steady pace, independent of its concentration. The Higuchi model showed a moderate fit (R^2 = 0.8483), suggesting that diffusion also plays a role in the release mechanism. In contrast, the first-order model showed the lowest correlation (R^2 = 0.7681), indicating it is the least suitable. These results confirm that PF3 provides controlled and sustained drug release, primarily governed by zero-order kinetics, which is ideal for maintaining consistent therapeutic levels. The details are shown in Figures 4 and 5.

Table 5: *In vitro* dissolution study

***In vitro* dissolution study of PF1–PF6**						
Time (HR)	**PF1**	**PF2**	**PF3**	**PF4**	**PF5**	**PF6**
0	0	0	0	0	0	0
1	6.33±0.12	7.26±0.54	11.50±0.03	10.86±0.98	6.10±0.96	6.39±0.09
2	13.33±0.02	21.47±0.23	21.49±0.75	14.81±0.42	22.62±0.87	15.07±0.78
3	22.87±0.04	26.75±0.85	26.78±0.86	19.01±0.06	26.40±0.92	20.91±0.35
4	34.32±0.06	34.91±0.45	34.94±0.06	26.84±0.89	31.43±0.05	26.83±0.42
5	34.62±0.08	52.12±0.23	52.14±0.74	31.87±0.48	37.76±0.09	45.96±0.87
6	63.85±0.01	63.32±0.06	63.35±0.06	61.01±0.32	63.28±0.632	72.81±0.04
7	86.79±0.03	75.28±0.98	75.31±0.04	80.16±0.12	72.68±0.42	79.54±0.09
8	91.73±0.13	86.03±0.75	97.09±0.63	84.49±0.05	88.88±0.08	86.54±0.02

***In vitro* dissolution study of PF7–PF12**							
Time (HR)	**PF7**	**PF8**	**PF9**	**PF10**	**PF11**	**PF12**	**PF13**
0	0	0	0	0	0	0	0
1	10.86±0.02	10.28±0.96	6.27±0.98	7.03±0.04	6.21±0.06	7.03±0.98	8.42±0.12
2	21.08±0.63	13.12±0.25	22.22±0.06	20.42±0.23	14.38±0.08	13.74±0.02	21.36±0.09
3	25.49±0.45	19.64±0.36	26.40±0.35	25.87±0.89	20.38±0.69	22.06±0.96	26.12±0.63
4	34.52±0.06	27.99±0.02	33.63±0.48	34.50±0.23	26.76±0.02	38.15±0.63	30.68±0.52
5	52.53±0.98	34.42±0.63	40.26±0.62	46.30±0.96	34.57±0.47	43.71±0.05	40.72±0.08
6	70.53±0.05	46.16±0.45	51.52±0.12	56.66±0.78	52.65±0.69	56.02±0.96	43.96±0.05
7	68.19±0.03	58.14±0.78	80.13±0.02	72.76±0.38	59.79±0.52	61.67±0.09	53.27±0.14
8	91.44±0.14	84.24±0.21	85.34±0.35	92.15±0.78	93.45±0.21	89.65±0.48	84.50±0.05

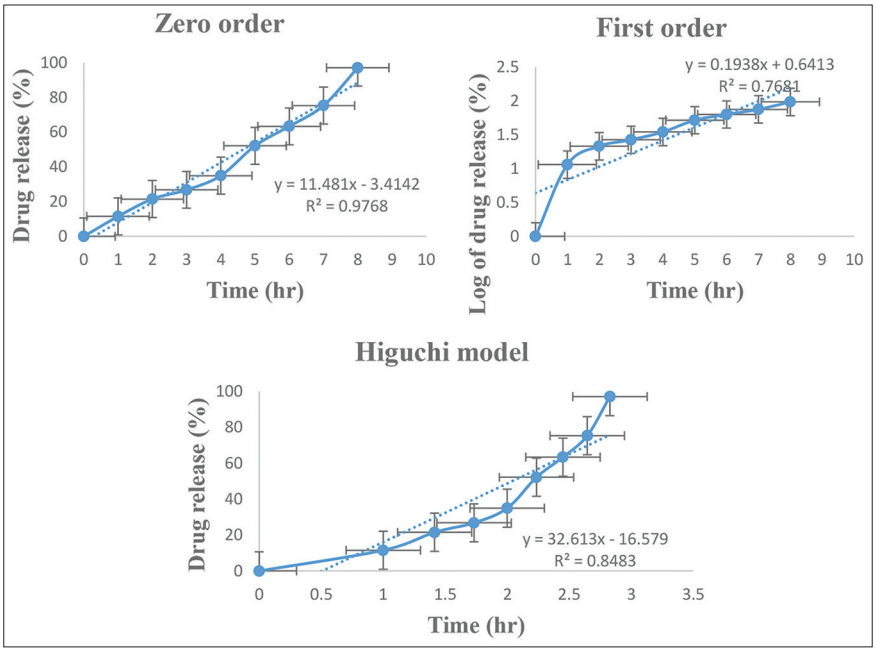

Figure 4: Zero-order, first-order, and Higuchi model of PF3

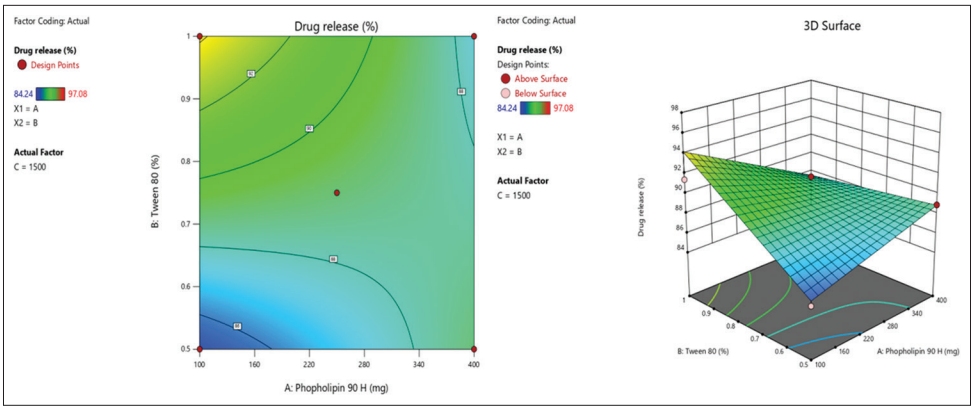

Figure 5: Counter and 3d plots of drug release kinetics

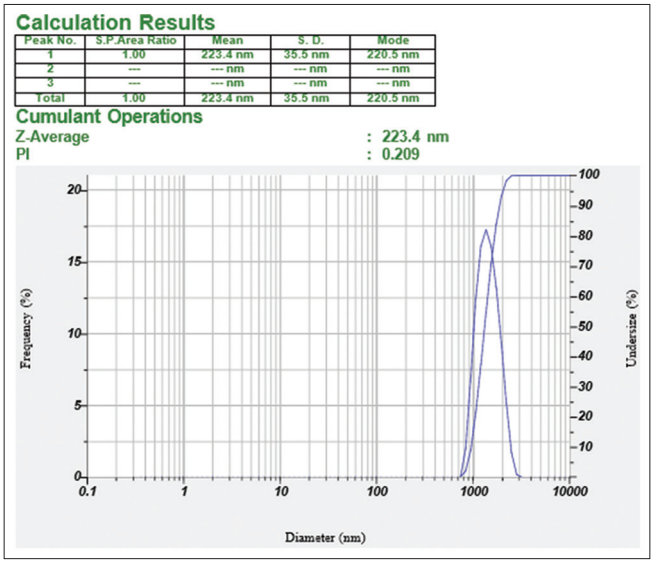

Figure 6: Particle size and polydispersity index of PF3

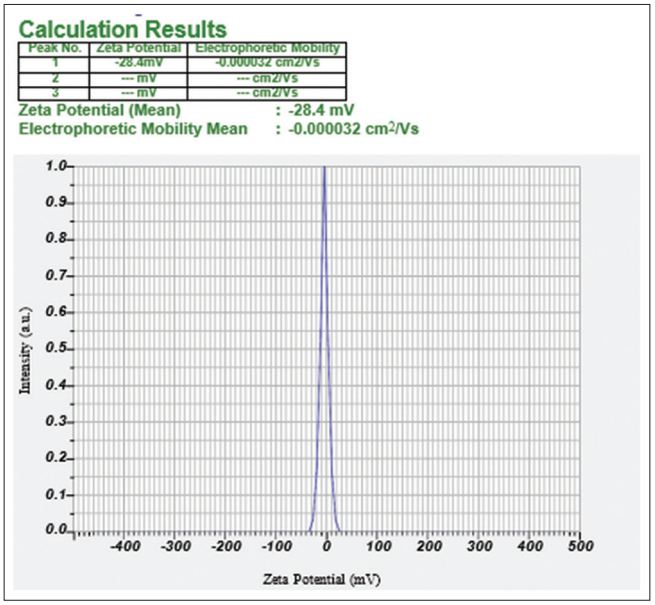

Figure 7: Zeta potential of PF3

Particle size, PDI, and zeta potential

Ranged from 223.4 nm (PF3) to 425.5 nm (PF12), with PF3 exhibiting the smallest size, which may contribute to improved cellular uptake. The PDI values were within an acceptable range (<0.5), indicating relatively uniform particle distribution, with PF3 (0.209) and PF2 (0.219) showing the highest homogeneity shown in figure 6. The zeta potential values were negative for all formulations, ranging from −28.4 mV (PF3) to −15.7 mV (PF12), and suggesting moderate to good colloidal stability. Among the tested formulations, PF3 demonstrated the most favorable characteristics, with the smallest particle size, low PDI, and high zeta potential, making it a promising candidate for further development. The Zeta potential of PF3 is shown in figure 7.

Table 6: FTIR interpretation of PF3

Functional group	Observed wavenumber (cm^{-1})	Reported range (cm^{-1})
O–H stretch (carboxylic acids)	2853.17	3300–2500
C–C stretch (in–ring) (aromatic)	1487.51	1500–1400
C–H (alkane)	1351.86	1370–1350
C–N stretch (aromatic amines)	1310.38	1335–1250
C–O stretch	1292.07, 1117.55,	1320–1000
=C–H bend (alkenes)	861.06,767.53, 806.99	1000–650

FTIR: Fourier transform infrared

FTIR spectroscopy

The FTIR analysis, as per Figure 8, reveals the presence of key functional groups in the compound. The O–H stretch of carboxylic acids appeared at 2853.17/cm, within the 3300–2500/cm range. Aromatic C–C stretch was noted at 1487.51/cm, while alkane C–H stretch appeared at 1351.86/cm. A C–N stretch for aromatic amines was observed at 1310.38/cm the last values shows in table 6. C–O stretching vibrations were seen at 1292.07 and 1117.55/

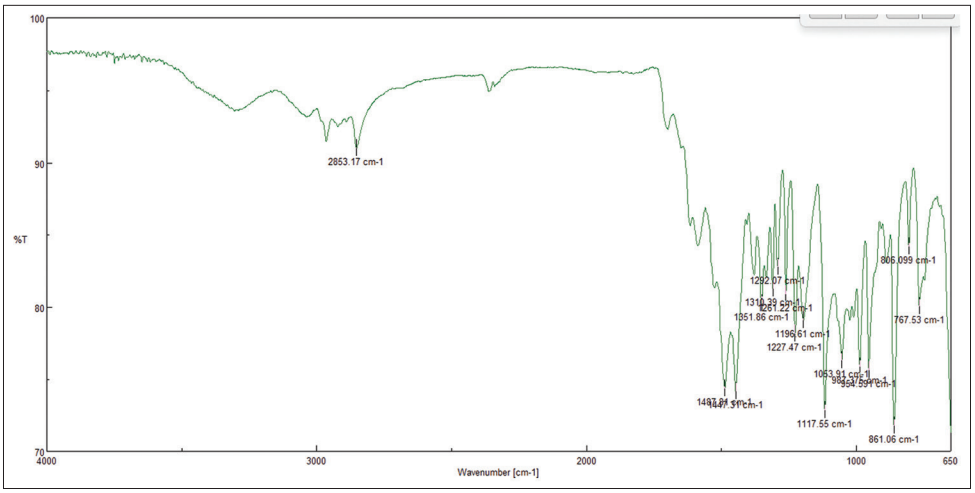

Figure 8: Fourier transform infrared spectrum of PF3

cm, and =C–H bending of alkenes was identified at 861.06, 806.99, and 767.53/cm. These peaks confirm the presence of carboxylic acid, aromatic ring, alkane, aromatic amine, ether/ester, and alkene functionalities.

DSC

Figure 9 shows the DSC thermogram of PF3, which has a prominent endothermic peak at 192.47°C. The peak starts at 191.41°C and ends at 195.29°C. This sharp melting peak is a strong indication of the crystalline nature of PF3, as crystalline materials typically show distinct melting transitions, unlike amorphous substances, which display broad glass transition events. The well-defined peak suggests a high degree of molecular order, confirming that PF3 exists in a crystalline state.

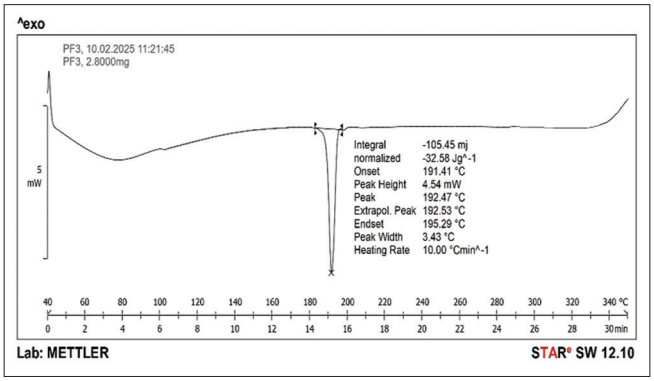

Figure 9: Differential scanning calorimetry thermogram of PF3

XRD

Figure 10 shows the XRD study reveals distinct differences between pure DTG and its optimized formulation PF3. Pure DTG exhibits a predominantly amorphous nature, as indicated by a broad halo and diffused, low-intensity peaks in its diffractogram. Minor peaks are observed at 2θ values of 15.2°, 16.9°, 18.3°, 20.1°, 22.3°, 24.3°, 27.2°, 27.6°, 29.1°, and 35.2°, but these are not sharp or intense enough to suggest significant crystallinity, confirming the absence of long-range molecular order. In contrast, The XRD pattern of PF3 has clear and strong peaks at 2θ values of 14.2°, 18.9°, 19.5°, 22.7°, 23.8°, 25.9°, and 28.3°, indicating a crystalline nature. This transformation from amorphous to crystalline form in PF3 suggests successful formulation modification, potentially improving the drug's physicochemical stability and performance.

SEM

The picture of DTG in SEM in Figure 11 reveals a heterogeneous mixture of particles with varying shapes and sizes, indicating a non-uniform surface morphology. The particles appear mostly irregular and aggregated, with sizes ranging from approximately 56.9 nm to 122.3 nm as marked in the image. The surface texture is rough, suggesting possible amorphous characteristics in line with the XRD results. The SEM picture of PF3 shows that there are nanoparticles with diameters between 53.14 nm and 590.4 nm. These Nano sized structures suggest a high surface area, which may enhance solubility and bioavailability. The observed morphology shows well-defined Nano rods and partially aggregated nanoparticles, which could influence the formulation's stability and performance. Figure 11 shows a SEM image of PF3 that shows nanoparticles that are between 53.14 nm and 590.4 nm in size. These Nano sized structures suggest a high surface area, which may enhance solubility and bioavailability. The observed morphology shows well-defined Nano rods and partially aggregated nanoparticles, which could influence the formulation's stability and performance.

Stability study

The stability study mentioned in Table 7 of the optimized batch PF3 over a 3-month period demonstrated excellent

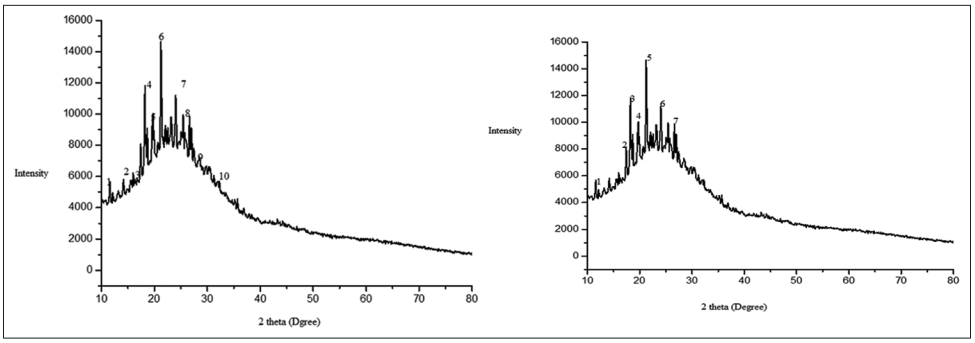

Figure 10: X-ray diffraction images of Dolutegravir and X-ray Diffractogram of PF3optimised batch

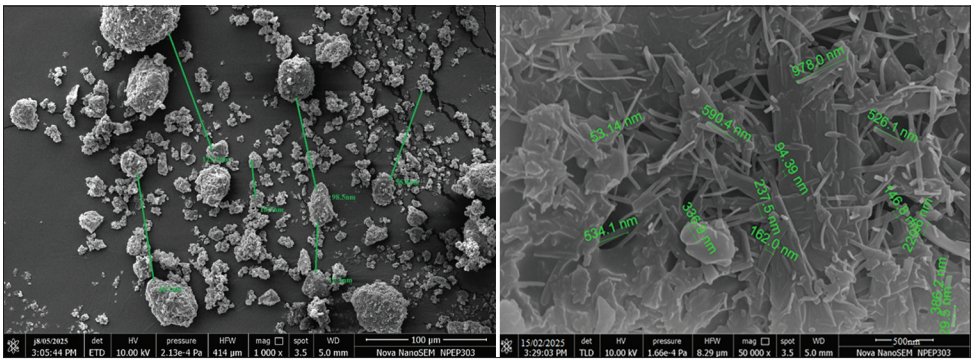

Figure 11: Scanning electron microscopy images of Dolutegravir and PF3

Table 7: Stability study of optimized batch PF3

Parameter	Initial	1	2	3
Drug content (%)	97.34±0.36	97.30±0.12	97.29±0.30	97.25±0.01
Entrapment efficiency (%)	93.94±0.63	93.93±0.53	93.90±0.03	93.90±0.01
Drug release (%)	97.09±0.63	97.07±0.052	97.05±0.15	97.04±0.01

consistency in formulation performance. The drug content remained stable, showing only a minimal decrease from 97.34% initially to 97.25% at the end of the 3rd month, indicating good chemical stability of the active ingredient. EE% also remained virtually unchanged, with values ranging narrowly from 93.94% to 93.90%, confirming the robustness of the encapsulation process. Similarly, drug release showed negligible variation, decreasing slightly from 97.09% to 97.04%, which signifies sustained release properties without significant degradation or formulation instability. Overall, the results suggest that PF3 maintains its integrity, effectiveness, and controlled release profile throughout the study period, supporting its suitability for long-term pharmaceutical use.

CONCLUSION

The present study examined how to optimize DTG -loaded SLNs using the hot homogenization method along with ultrasonication. A Box-Behnken design under RSM helped explore the effects of three important independent variables: Lipid concentration (Phospholipon 90 H), surfactant concentration (Tween 80), and homogenization speed. Thirteen formulations (PF1–PF13) were created with different levels of these variables. We examined each formulation for drug content, how well it trapped drugs, and how well it released drugs *in vitro*.

PF3 showed the best results, with the highest drug content (97.34%) and EE% (93.94%), making it the most promising option for further development. Statistical analysis, backed by analysis of variance, confirmed that the chosen formulation variables significantly influenced the key quality features of the SLNs. The quadratic response surface models created were solid and predictive, indicating they could be useful for making other SLN-based drug delivery systems.

The findings suggest that carefully optimizing formulation components, such as lipid and surfactant concentrations, along with processing conditions, such as homogenization speed, can greatly improve the properties of SLNs. For PF3, these optimized conditions led to better drug encapsulation and release characteristics, which are essential for enhancing therapeutic effectiveness. In general, the study shows how helpful RSM may be in careful planning and development of SLN formulations and offers a practical approach for

improving the delivery of DTG and possibly other lipophilic drugs using nanoparticulate systems.

REFERENCES

1. Mühlen AZ, Schwarz C, Mehnert W. Solid lipid nanoparticles (SLN) for controlled drug delivery--drug release and release mechanism. Eur J Pharm Biopharm 1998;45:149-55.
2. Cavalli R, Caputo O, Gasco MR. Solid lipospheres of doxorubicin and idarubicin. Int J Pharm 1993;89:R9-12.
3. Müller RH, Dingler A, Schneppe T, Gohla S. Large scale production of solid lipid nanoparticles (SLN™) and nanosuspensions (DissoCubes™). Handb Pharm Control Release Technol 2000;14:359-76.
4. Mulla JS, Khazi IM, Jamakandi VG. Solid lipid nanoparticles: Potential applications. Indian J Nov Drug Deliv 2010;2:82-7.
5. Swathi G, Prasanthi NL, Manikiran SS, Ramarao N. Solid lipid nanoparticles: Colloidal carrier systems for drug delivery. Int J Pharm Sci Res 2010;1:1-6.
6. Sarathchandiran I. A review on nanotechnology in solid lipid nanoparticles. Int J Pharm Dev Technol 2012;2:45-61.
7. Prasanth Y, Madhusudhan S, Rasheed SH, Lakshmi PV. Design and characterization of dolutegravir sodium loaded solid lipid nano particles. J Drug Alcohol Res 2023;12:102441.
8. Faria MJ, Lopes CM, Das Neves J, Lúcio M. Lipid nanocarriers for anti-HIV therapeutics: A focus on physicochemical properties and biotechnological advances. Pharmaceutics 2021;13:1294.
9. Bhalekar M, Upadhaya P, Madgulkar A. Formulation and characterization of solid lipid nanoparticles for an anti-retroviral drug darunavir. Appl Nanosci 2017;7:47-57.
10. Gupta S, Kesarla R, Chotai N, Misra A, Omri A. Systematic approach for the formulation and optimization of solid lipid nanoparticles of efavirenz by high pressure homogenization using design of experiments for brain targeting and enhanced bioavailability. Biomed Res Int 2017;2017:5984014.
11. Tian W, Han S, Huang X, Han M, Cao J, Liang Y, *et al*. LDH hybrid thermosensitive hydrogel for intravaginal delivery of anti-HIV drugs. Artif Cells Nanomed Biotechnol 2019;47:1234-40.
12. Sangeetha S. Formulation design, optimization, and evaluation of solid lipid nanoparticles loaded with an antiviral drug tenofovir using box-behnken design for boosting oral bioavailability. Adv Pharmacol Pharm Sci 2024;2024:5248746.
13. Castelli F, Puglia C, Sarpietro MG, Rizza L, Bonina F. Characterization of indomethacin-loaded lipid nanoparticles by differential scanning calorimetry. Int J Pharm 2005;304:231-8.
14. Yadav V, Alok M, Prajapati S, Alok S, Verma A, Kumar A, *et al*. Solid lipid nanoparticles (sln): Formulation by high pressure homogenization. World J Pharm Pharm Sci 2014;3:1200-13.
15. Padhye SG, Nagarsenker MS. Simvastatin solid lipid nanoparticles for oral delivery: Formulation development and *in vivo* evaluation. Indian J Pharm Sci 2013;75:591-8.
16. Shaikh NA, Lala RR. Formulation development of dolutegravir sodium loaded nano lipid carriers for improved solubility and permeability. Int J Pharm Sci Res 2021;12:3654-65.
17. Singh S, Dobhal AK, Jain A, Pandit JK, Chakraborty S. Formulation and evaluation of solid lipid nanoparticles of a water soluble drug: Zidovudine. Chem Pharm Bull (Tokyo) 2010;58:650-5.
18. Nachammai K, Nair KG, Velmurugan R, Pavithra SK. Sustained - release study on mefenamic acid and mosapride loaded solid lipid nanoparticles: *In vitro* characterization. Res J Pharm Technol 2020;13:5391-5.
19. Manjunath K, Venkateswarlu V. Pharmacokinetics, tissue distribution and bioavailability of clozapine solid lipid nanoparticles after intravenous and intraduodenal administration. J Control Release 2005;107:215-28.
20. Vyas SP, Khar RK. Controlled Drug Delivery Concepts and Advances. Vol. 1. Delhi: Vallabh Prakashan; 2002. p. 411-47.
21. AlHaj NA, Abdullah R, Ibrahim S, Bustamam A. Tamoxifen drug loading solid lipid nanoparticles prepared by hot high pressure homogenization techniques. Am J Pharmacol Toxicol 2008;3:219-24.
22. Shi F, Zhao JH, Liu Y, Wang Z, Zhang YT, Feng NP. Preparation and characterization of solid lipid nanoparticles loaded with frankincense and myrrh oil. Int J Nanomedicine 2012;7:2033-43.
23. Iqbal A, Zaman M, Amjad MW, Adnan S, Raja MA, Rizvi SF, *et al*. Solid lipid nanoparticles of mycophenolate mofetil: An attempt to control the release of an immunosuppressant. Int J Nanomedicine 2020;15:5603-12.
24. Babu VN, Rao GS, Budha RR, Alavala RR, Desu PK, Babu GK, *et al*. Development, characterization and optimization of solid lipid nanoparticles of alpha-mangostin by central composite design approach. J Appl Pharm Sci 2023;13:140-50.
25. Müller RH, Runge SA, Ravelli V, Thünemann AF, Mehnert W, Souto EB. Cyclosporine-loaded solid lipid nanoparticles (SLN): Drug-lipid physicochemical interactions and characterization of drug incorporation. Eur J Pharm Biopharm 2008;68:535-44.

Source of Support: Nil. **Conflicts of Interest:** None declared.